

Check for updates

Neuroscience Research



# Modulation of Hypothalamic Dopamine Neuron Activity by Interaction Between Caloric State and Amphetamine in Zebrafish Larvae

Pushkar Bansal<sup>1</sup> 🕞 | Mitchell F. Roitman<sup>2</sup> | Erica E. Jung<sup>1,3</sup>

<sup>1</sup>Department of Mechanical and Industrial Engineering, The University of Illinois at Chicago, Chicago, Illinois, USA | <sup>2</sup>Department of Psychology, The University of Illinois at Chicago, Chicago, Illinois, USA | <sup>3</sup>Department of Bioengineering, The University of Illinois at Chicago, Chicago, Illinois, USA

Correspondence: Erica E. Jung (ejung72@uic.edu)

Received: 5 March 2024 | Revised: 24 June 2024 | Accepted: 20 October 2024

Edited by Junie Paula Warrington and Samantha McLean. Reviewed by Frederick E. Williams.

Funding: This work was supported by National Science Foundation (CBET 2309589) and National Institutes of Health (DA025634).

Keywords: amphetamine | calcium imaging | dopamine | food deprivation | hypothalamus | reward | zebrafish larva

# **ABSTRACT**

Dopamine (DA) signaling is evoked by both food and drugs that humans come to abuse. Moreover, physiological state (e.g., hunger versus satiety) can modulate the response. However, there is great heterogeneity among DA neurons. Limited studies have been performed that could resolve the interaction between physiological state and drug responsivity across groups of DA neurons. Here, we measured the activity of neurons in transgenic Tg (th2:GCaMP7s) zebrafish larva that expresses a calcium indicator (GCaMP7s) in A11 (posterior tuberculum) and a part of A14 (caudal hypothalamus and intermediate hypothalamus) DA populations located in the hypothalamus of the larval zebrafish. Fish were recorded in one of two physiological states: ad-libitum fed (AL) and food deprived (FD) and before and after acute exposure to different doses of the stimulant drug amphetamine (0, 0.7, and  $1.5\,\mu$ M). We quantified fluorescence change, activity duration, peak rise/fall time, and latency in the calcium spikes of the DA neurons. Our results show that baseline DA neuron activity amplitude, spike duration, and correlation between inter- and intra-DA neurons were higher in the FD than in the AL state. Dose-dependent AMPH treatment further increased the intensity of these parameters in the neuron spikes but only in the FD state. The DA activity correlation relatively increased in AL state post-AMPH treatment. Given that hunger increases drug reactivity and the probability of relapse to drug seeking, the results support populations of DA neurons as potential critical mediators of the interaction between physiological state and drug reinforcement.

# 1 | Introduction

Drugs that humans come to abuse increase dopamine concentration in dopamine terminal regions (Di Chiara and Imperato 1988). However, the mechanisms by which increased extracellular dopamine levels are achieved vary across drugs (Wei et al. 2018). Amphetamine (AMPH) is one of the most widely used and abused substances (Kramer, Fischman, and Littlefield 1967). Yet, its mechanism(s) of action remains controversial (Siciliano et al. 2014). Along similar lines,

food restriction enhances the dopamine response to food (Cone, Mccutcheon, and Roitman 2014; Wilson et al. 1995), but food restriction modulates dopamine signaling in various ways (Branch et al. 2013; Geisler and Hayes 2023; Liu and Borgland 2015). Finally, it is critical to note that there is an interaction between physiological states (e.g., food restriction, satiety) and drug behavioral reactivity with food deprivation/restriction particularly affecting responses to amphetamine (Bansal, Roitman, and Jung 2023; Campbell and Fibiger 1971; Deroche et al. 1993). It remains unknown

This is an open access article under the terms of the Creative Commons Attribution-NonCommercial-NoDerivs License, which permits use and distribution in any medium, provided the original work is properly cited, the use is non-commercial and no modifications or adaptations are made.

© 2024 The Author(s). Journal of Neuroscience Research published by Wiley Periodicals LLC.

# **Summary**

- External stimuli including caloric states (e.g., fooddeprivation and feeding) and drugs of abuse (e.g., amphetamine) are known to alter the dynamics of mesolimbic reward circuitry in the mammalian brain.
- In this novel study, we demonstrated the individual and interactive effects of these stimuli in larval zebrafish where amphetamine treatment in food-deprived zebrafish induced a region-specific increase in activity of dopaminergic neurons than the satiated counterparts.
- Our results could aid in developing interventions in different drug intake scenarios by modifying diet and thereby controlling dopaminergic activity.

how food deprivation/restriction may interact with the different proposed mechanisms of amphetamine action. Here, we investigate the interaction between caloric state and amphetamine on the firing rate of dopamine neurons.

In mammals, several different populations of dopaminergic (DA) neurons (A8-A16) have been identified (Björklund and Dunnett 2007). Within these populations, there is a growing body of literature supporting transcriptional (Phillips et al. 2022) and functional (Engelhard et al. 2019; Morales and Margolis 2017) heterogeneity. Some of these populations (e.g., A8) are involved in controlling motivation and emotional behavior (Fiorenzano et al. 2021), and others (e.g., A9 and A10 regions) play key roles in reward and reinforcement (Ikemoto 2010; Schultz 2002), drug reactivity and the development of addiction. While the Periventricular A11 region contributes to pain modulation (Charbit et al. 2009) and restless leg syndrome (Clemens 2006). Energy homeostasis is controlled by two distinct DA populations (A12 and A13) (Ye, Nunez, and Zhang 2023; Zhang and Van Den Pol 2016), whereas motor activity is largely controlled by the A11 (Koblinger et al. 2014) and A14 regions (Korchynska et al. 2022), and odor discrimination and processing are modulated by the A16 region (Capsoni et al. 2021). These behaviors result from dopamine neuron activation, and the dopamine activity is generally increased by amphetamine (Calipari and Ferris 2013). However, dopamine activity in only a few of these regions (e.g., A9, A10, A11, and A14) (Fougère et al. 2019; Giros et al. 1996; Koblinger et al. 2014; Koirala, Shah, and Khanal 2014; Ryczko and Dubuc 2017; Vezina 1988) has been directly studied in response to amphetamine, whereas in A14 region, amphetamine showed an indirect change in DA activity (Korchynska et al. 2022). Moreover, contradictory response in the A9 (Bernardini et al. 1991; Fougère et al. 2019; Koirala, Shah, and Khanal 2014) region has been observed in response to amphetamine, and nearly half of the remaining DA regions (A8, A15, A13, and A16) were unexplored.

DA populations in the brain are highly conserved across different animal species, including zebrafish (Barrios et al. 2020; Wasel and Freeman 2020). Here, we used larval zebrafish, a vertebral teleost, to investigate the dopaminergic responses to food deprivation and a stimulant drug (AMPH). Zebrafish is a vertebral animal model gaining momentum in neuroscience

research, especially due to their highly conserved brain structure and genome compared to mammals. Its small size (~3 mm) makes it easy to house for raising and handling during experimentation. Zebrafish larvae are optically transparent, which is advantageous in imaging and recording the activities inside the larval body, such as in the heart and brain (Bansal, Roitman, and Jung 2023; Keller and Ahrens 2015). We leveraged all these useful features, including optical transparency in the larvae, and recorded the change in DA neuron activity at a single neuron level using calcium imaging in vivo in real time. To accomplish this, we used 6dpf larvae of a transgenic zebrafish line Tg(th2:GCaMP7s) expressing fluorescent activity in A11 (PT) and A14 (cH, iH) DA neurons in its hypothalamus. We treated the larvae with two different doses of AMPH (0.7 and 1.5 µM) while they were in ad libitum fed (AL) and food-deprived (FD) state. We hypothesized that amphetamine would increase activity in all three DA populations in FD states than in fed states. Our results show that food deprivation alone and its interaction with amphetamine increased dopamine neuron firing relative to the fed state. Impairment in correlation among dopamine regions in food-restricted state was also observed in post-AMPH treatment. Collectively these data show the effect of hunger-AMPH interaction in modulating the activity in different dopaminergic regions.

# 2 | Materials and Methods

# 2.1 | Zebrafish Maintenance

Parent transgenic zebrafish line Tg(th2:GCaMP7s) was outsourced and raised in our fish facility at the University of Illinois at Chicago. All adult fish tanks were stacked in the fish racking system (Aquaneering Inc., San Diego, CA). The experiments conducted here were approved by the Association for Assessment and Accreditation of Laboratory Animal Care (AAALAC). All zebrafish larvae used here were 6dpf and were kept in the fish facility till they turned 6dpf. The fish facility was maintained at 28°C with a 14/10 h light/dark cycle. The fish rack that constituted the fish water was maintained with a conductivity range of 600–800 μs and a pH range of 7.2–7.8.

# 2.2 | Experimental Groups

The larvae were divided into two feeding groups: ad libitum (AL, n=20) and FD (n=18). Experimental subjects from each group were picked at random to minimize any subject bias. Sample size analysis was not performed however, we used the size based on the best studies published previously related to neural imaging in this animal model (Kappel et al. 2022; Kim et al. 2017). Larvae that failed to elicit any detectable response or were physiologically abnormal were excluded from the study and analysis. Ad libitum larvae had unrestricted access to food since they turned 5dpf until the experimentation. FD larvae were never fed at any stage of raising and experimentation. Sex determination of the subjects cannot be performed at this stage since it can be done between 20 and 25 of larval age (Kossack and Draper 2019). Both feeding groups were treated with two different doses of amphetamine (AL 0.7 µM, AL 1.5 µM, and FD  $0.7 \mu M$ , FD  $1.5 \mu M$ ). Initial dopamine neuron recording was performed for five continuous minutes in fish water (without amphetamine). After 5 min, the recording was stopped, and fish water was pipetted out and replaced with amphetamine solution. The neuron recording was again performed for another 5 min.

# 2.3 | Sample Preparation and Recording Material

For recording DA neuron activity, the individual larva was first paralyzed using 30 µL of 300 µM stock pancuronium bromide (YC10036-1, 10MG, Millipore Sigma, WI, USA) to prevent any unwanted muscle twitching in the larvae to avoid error in recordings. After paralysis, larvae were completely immobilized in a 1.5% agarose gel solution drop and were covered with 0.5 mL fish water for 5 min baseline recording. After Baseline recording, the fish water was pipetted out and replaced with 0.5 mL d-amphetamine hemisulfate solution (Sigma Aldrich, MO). The drug was allowed to seep through the agarose drop for ~5 min, and treatment recording was commenced for 5 min again. We used a 40× water immersion objective to visualize and record the neuron (40×/0.80W, Olympus Corporation, Japan) mounted on an upright epifluorescence microscope setup consisting of a fluorescence excitation and illumination setup (X-cite 120 series, Excelitas Technologies Corp., Canada). The microscope was equipped with a GFP filter with 488nm excitation/507nm emission (Chroma Technology Corp, VT). The setup was connected to an image visualization software (HC Image Live, Hamamatsu Photonics, Japan). The recording was made at 10 ms exposure time with 35 frames per second. Recordings were opened in ImageJ, and a complete neuron cluster (approx. n = 3-7 visible neurons/larva/DA population) (Figure 1a) was selected from all three populations separately in the same frame using a polygon ROI tool along the edges of the cluster to avoid surrounding noisy regions.

# 2.4 | Post Processing

The data from ImageJ were extracted as intensity versus frames, and frames were converted into time in Microsoft Excel. Newly generated time versus intensity data were exported to OriginPro (Version 2022, OriginLab Corporation, Northampton, MA, USA). The Data were divided population-wise and were first smoothened (F) using an FFT filter (window points = 30). A baseline (Fo) was created from the smoothened intensity data using an inbuilt function called "peak analysis" from the analysis tab using an asymmetric least squares smoothing algorithm by varying parameters suitable for the data. The baseline data were subtracted from smoothened intensity data and divided by baseline data ( $\frac{df}{f}F-Fo/Fo$ ). The  $\frac{df}{f}$  values were opened again with the peak analysis function, and the peak integration function was used to obtain peak count and left and right half peak width values. The latency was calculated by subtracting two subsequent time points from the peaks (peak height threshold:  $\geq$  10% of d*f/f*; local points = 2) (Figure 1b).

# 2.5 | Statistical Analysis

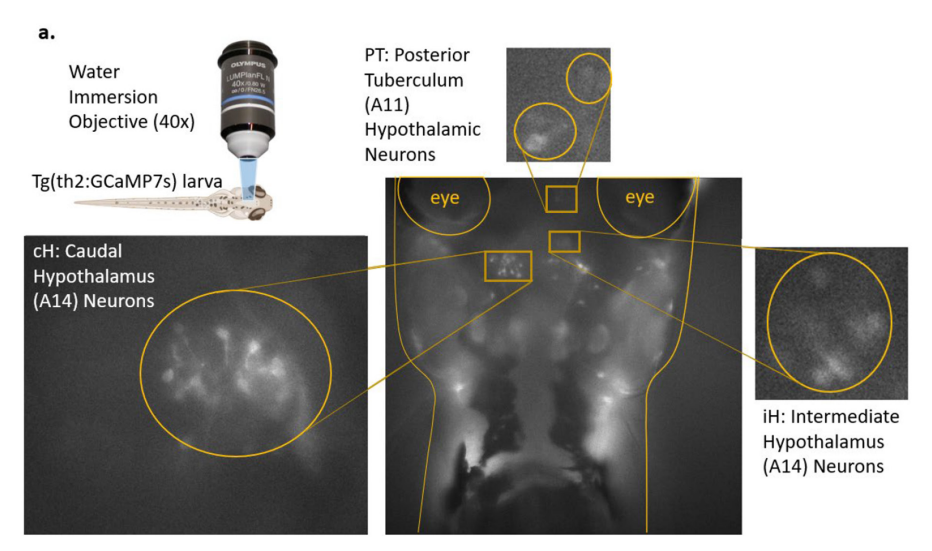
All data were statistically analyzed using OriginPro. Data were checked for normality and were found to be rejecting normality. For Baseline analysis, a non-parametric test, the Mann-Whitney

U test for independent samples, was used between two data sets. Kruskal–Wallis ANOVA was performed for dose-dependent and latency analysis, followed by Dunn's post hoc analysis. Correlation analysis was performed using Spearman Correlation. All significantly different data are shown with p < 0.05 with exact p values and no significance was shown for non-significant p-value (p > 0.05, also shown with exact p values). All the outliers were excluded from the statistical analysis. Box plot limits are represented as Q1–Q3: 25%–75%, and whiskers are represented by outliers (1.5QR). The black horizontal line within the box represents the median with values mentioned on the right side of the line, and the black dot represents the mean of the data.

## 3 | Results

# 3.1 | Food Deprivation Increases Baseline Dopamine Activity in the Hypothalamus

Feeding states alter dopaminergic activity in animals. Here, we examined how food deprivation alters the dopaminergic activity in different brain regions in zebrafish larvae. In Figure 2a-c, we compared the peak amplitude between ad libitum (AL) and FD groups in three distinct dopaminergic neuron populations in the hypothalamus (cH, caudal hypothalamus; iH, intermediate hypothalamus; PT, posterior tuberculum). With the statistical comparison of the peak amplitude data, we found that food deprivation increased the fluorescence activity in all three DA neuron populations with prominence in cH neurons (median  $\Delta F/F$ o: AL: 0.94%; FD: 2.17%; Mann-Whitney U test: p < 0.001) followed by iH neurons (median  $\Delta F/F$ o: AL: 0.98%; FD: 1.46%; Mann-Whitney U test: p < 0.001) and PT neurons (median  $\Delta F/Fo$ : AL: 0.76%; FD: 1.21%; Mann–Whitney U test: p < 0.001). Furthermore, we also investigated the peak width, which represents the time the DA neurons took to show one whole spike in the form of a calcium trace (Figure 2d-f). We did not find a significant width difference in peaks between AL and FD larvae in cH neuron (median peak width: AL: 4.41s; FD: 4.63s; Mann-Whitney U test: p = 0.074); however, in both iH (median peak width: AL: 5.57 s; FD: 6.24 s; Mann–Whitney U test: p < 0.001) and PT neurons (median peak width: AL: 4.31s; FD: 4.55s; Mann–Whitney *U* test: p = 0.014), the peaks were significantly wider in FD state. In Figure 2g-i, we analyzed the left-half peak width of the calcium trace peaks that signify the time taken by the neuron activity peaks to reach the maximum amplitude beginning from the resting state. Here, statistical significance in left half peak width between AL and FD state can be found in all three DA neuron populations significantly in cH (median peak width: AL: 0.76s; FD: 0.82s; Mann-Whitney *U* test: p = 0.032), iH neurons (median peak width: AL: 0.714s; FD: 0.792s; Mann-Whitney *U* test: p < 0.001), and PT neurons (median peak width: AL: 0.76s; FD: 0.84s; Mann–Whitney *U* test: p < 0.001). Similarly, we also compared the difference in right-half peak width, showing the time the calcium peaks took to reach the resting state from the maximum amplitude. The right half peak width was higher in the FD state in all three DA neurons. The difference was greatest in iH population (median peak width: AL: 0.82s; FD: 0.93s; Mann–Whitney U test: p < 0.001) and then in PT neurons (median peak width: AL: 0.97 s; FD: 1.06 s; Mann–Whitney *U* test:



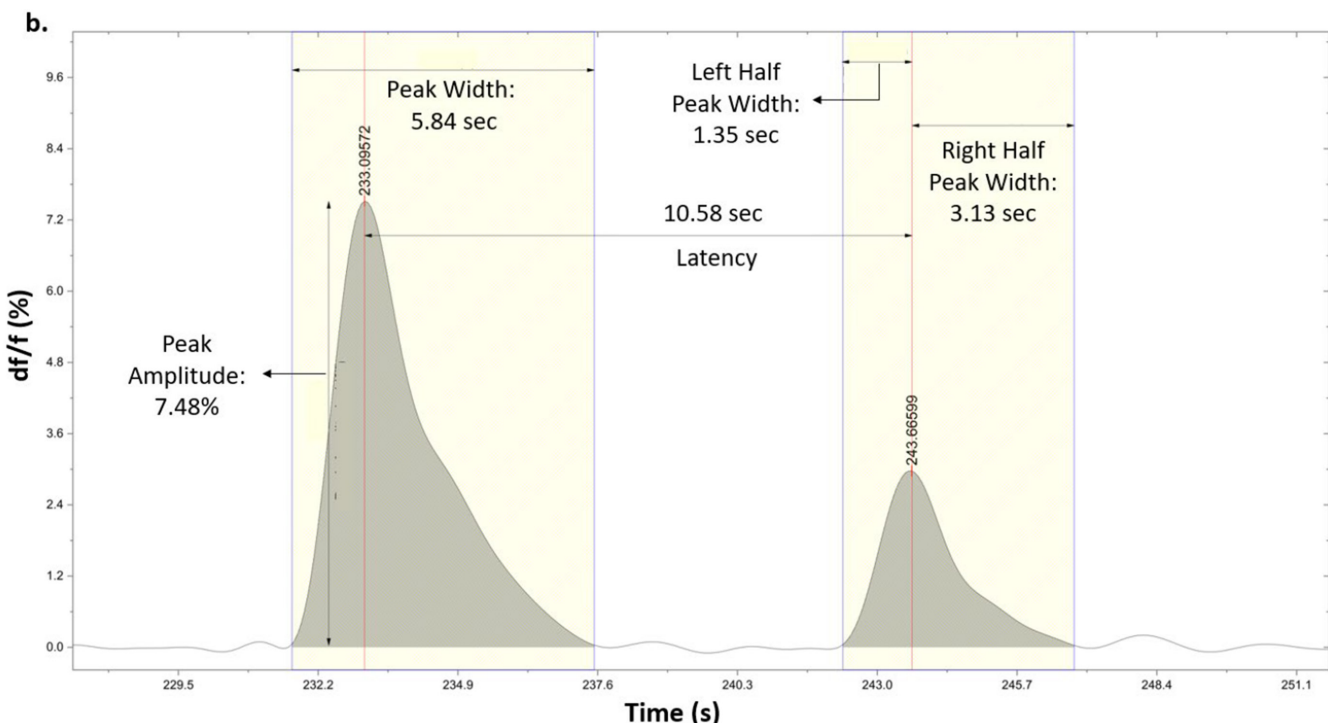


**FIGURE 1** | Larval imaging, dopamine neuron populations, and spike parameters. Calcium activity in three dopaminergic neuron populations (cH, iH, PT) in the hypothalamus of the transgenic larvae Tg(th2:GCaMP5) was analyzed with its characteristic parameters. (a) In the transgenic larvae, calcium activity in DA neurons in the caudal hypothalamic region, intermediate hypothalamic region, and the posterior tuberculum were recorded pre- and post-AMPH. The recording setup included a  $40\times$  water immersion objective connected to an epifluorescence microscope, and the individual larvae were paralyzed and immobilized in a drop of agarose. (b) In the calcium activity, five different parameters (df/f, peak width, left half peak width, right half peak width, and latency) were analyzed. The peak amplitude/normalized fluorescence change in the calcium activity was denoted by df/f; peak width denotes the activity duration of individual peaks, left half peak width denotes the peak rise time, and right half peak width represents the falling peak of the calcium peak. The latency between peaks denotes the time interval between two subsequent peaks.

p < 0.001) and lowest in cH neurons (median peak width: AL: 0.97 s; FD: 1.05 s; Mann–Whitney U test: p = 0.026).

# 3.2 | Varying AMPH Doses Selectively Exhibited Increased Calcium Trace Amplitude in DA Neuron Populations in Caloric States

Amphetamine targets dopaminergic neurons and increases their activity in the brain to induce a rewarding effect. Here, we investigated the effects of two doses of amphetamine (0.7 and  $1.5\,\mu\text{M}$ ) to gain insight into the reward-related functioning of the recently identified DA populations in the hypothalamus in zebrafish larvae. We compared the response in these neurons between AL and FD groups in the abovementioned AMPH doses. We first compared the calcium trace peak amplitude (fluorescence change) between feeding states in two doses using Kruskal–Wallis ANOVA (Figure 3a–c). Comparison made in cH neurons (Figure 3a) showed an overall significance ( $\chi_3^2$ =113.44; n=405 [AL\_0.7], n=387

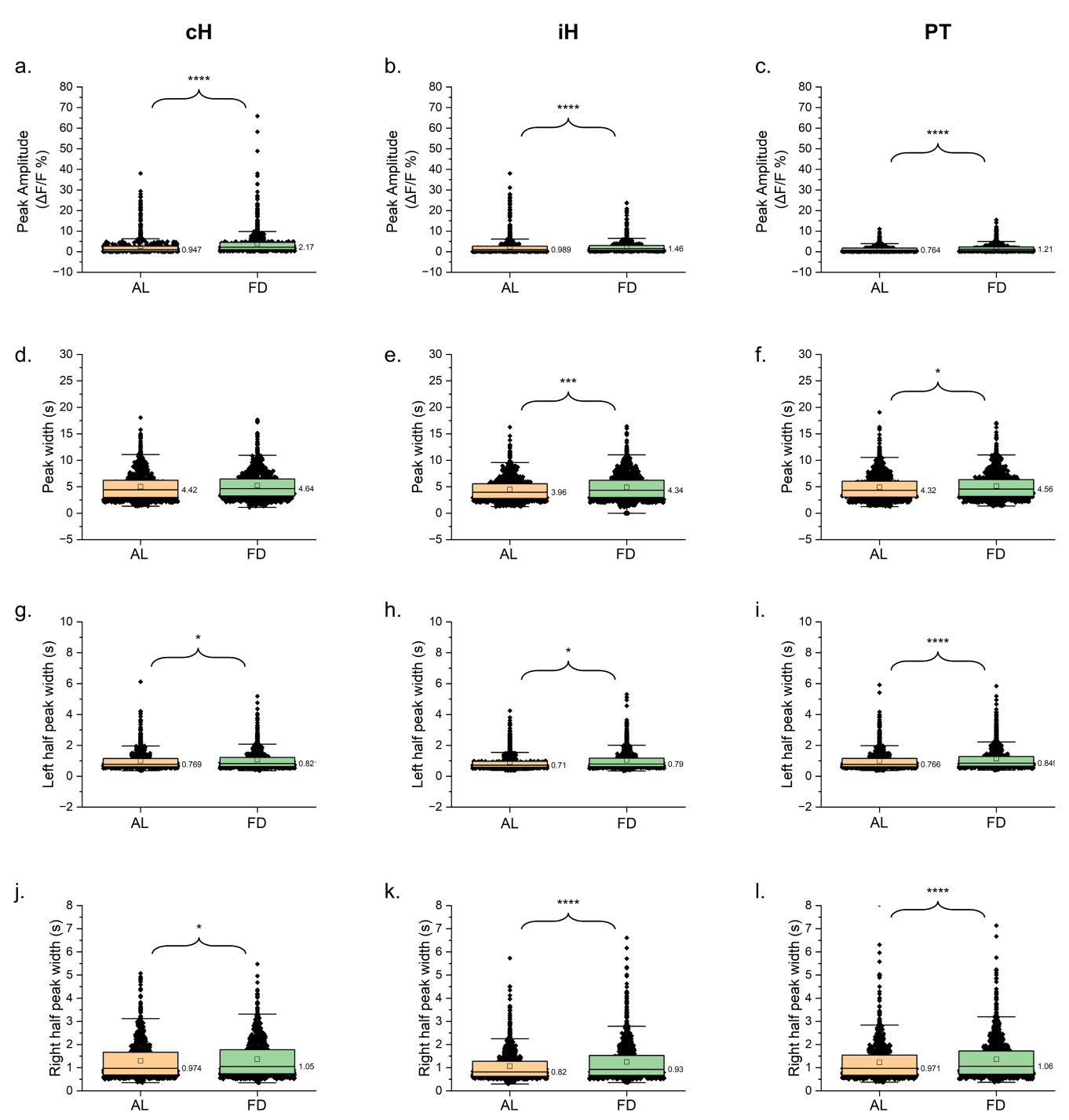


FIGURE 2 | Baseline activity analysis between states. Baselines between Ad libitum (AL, n = 20 fish) and food-deprived (FD, n = 18 fish) states were compared in four different calcium imaging data parameters that are peak amplitude (df/f)%, peak width, left half peak width, and right half peak width in three hypothalamic dopaminergic populations (caudal Hypothalamus [cH], intermediate Hypothalamus [iH], and posterior tuberculum [PT]) The data in all distribution are non-normal and thus tested using Mann–Whitney U test for independent data. (a–c) Fluorescence amplitude in neurons in untreated (baseline) state was significantly higher in the FD state than in the AL state in cH, iH, and PT (p < 0.001) (d–f) The fluorescence signal peak in baseline groups was significantly wider in FD larvae in iH (p < 0.001) and PT neurons only (p = 0.014) and mildly wider in cH and PT neurons. (g–i) Baseline left half peak widths were significantly wider in the FD state in all DA populations (cH: p < 0.005); iH, PT: p < 0.001). (j–l) Right half peak width was significantly higher in FD than in AL in all DA populations (cH: p = 0.026; iH: p < 0.001; PT: p < 0.001). Box plot limits are represented as Q1–Q3: 25%–75%, and whiskers are represented by outliers (1.5QR). The black horizontal line within the box represents the median with values mentioned on the right side of the line, and the blank square represents the mean of the data.

[FD\_0.7], n = 361 [AL\_1.5], n = 349 [FD\_1.5]; p < 0.001). Post hoc comparison indicated that both doses in the FD state showed an increased neuron fluorescence relative to the AL

state in cH population (median  $\Delta F/F$ 0: 0.7  $\mu$ M [AL: 1.22%; FD: 1.56%], p < 0.001; 1.5  $\mu$ M [AL: 0.819%; FD: 2.1%], p < 0.001). In Figure 3b, overall significant effect in iH neurons was

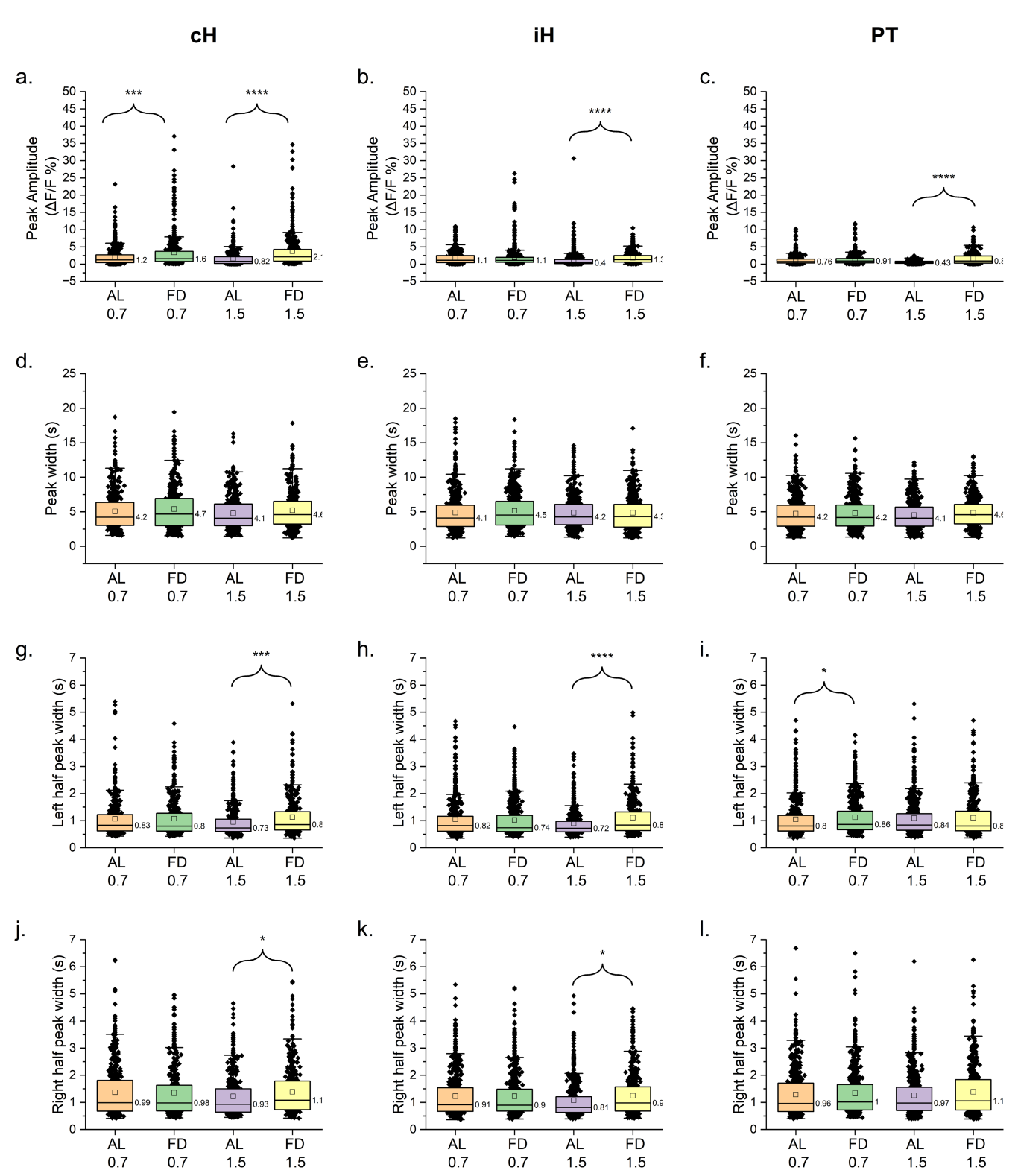


FIGURE 3 | Dose-dependent analysis between states. All four parameters were statistically analyzed at two different doses of amphetamine  $(0.7\,\mu\text{M} \, [\text{AL}: N=11; \text{FD}: N=10 \, \text{fish}] \, \text{and} \, 1.5\,\mu\text{M} \, (\text{AL}: N=9; \text{FD}: N=8 \, \text{fish}])$  and compared between AL and FD states using Kruskal–Wallis ANOVA for independent data followed by Dunn's post hoc comparison. Comparisons were made between AL and FD states in 0.7 and 1.5  $\mu$ M doses of AMPH in all three DA neuron populations. (a–c) Both doses  $(0.7 \, \text{and} \, 1.5\,\mu\text{M})$  increased cH fluorescence activity  $(0.7\,\mu\text{M}: p<0.001; 1.5\,\mu\text{M}: p<0.001)$  in cH neurons in FD state, and only 1.5  $\mu$ M AMPH dose increased neuron fluorescence in iH and PT populations (p<0.001). (d–f) Overall peak width did not change significantly across doses and states in all three DA populations. (g–i) Left half peak width was significantly larger in FD states only at 1.5  $\mu$ M AMPH dose in cH (p<0.001) and iH (p<0.001) and in AL state in PT neurons at  $0.7\,\mu$ M dose (p=0.027). (j–l) The right half peak was wider in the FD state at  $1.5\,\mu$ M in cH (p=0.028) and iH (p=0.016) population only. Box plot limits are represented as Q1–Q3: 25%–75%, and whiskers are represented by outliers  $(1.5\,0\text{R})$ . The black horizontal line within the box represents the median with values mentioned on the right side of the line, and the blank square represents the mean of the data.

observed ( $\chi_3^2$ =129.60; n=498 [AL\_0.7], n=485 [FD\_0.7], n=449 [AL\_1.5], n=424 [FD\_1.5]; p<0.001). Planned comparison showed a higher peak amplitude in FD state compared to AL state was observed only at 1.5 μM dose (median  $\Delta F/F$ o: 0.7 μM [AL: 1.12%; FD: 1.09%], p=1.000; 1.5 μM [AL: 0.40%; FD: 1.3%], p<0.001). Similar to the other two populations, Kruskal-Wallis ANOVA conveyed an overall significant difference in PT neurons ( $\chi_3^2$ =104.68; n=522 [AL\_0.7], n=513 [FD\_0.7], n=491 [AL\_1.5], n=379 [FD\_1.5]; p<0.001). Here, the peak amplitude of the calcium traces was found to be higher in FD larvae than in AL larvae at 1.5 μM dose only (median  $\Delta F/F$ o: 0.7 μM [AL: 0.76%; FD: 0.91%], p=0.475; 1.5 μM [AL: 0.43%; FD: 0.8%], p<0.001) (Figure 3c).

# 3.3 | Food Deprivation Potentiated Hypothalamic DA Activity by Increasing the Rising and Falling Duration of Calcium Peaks Post-AMPH Treatment

We investigated whether varying the AMPH dose affects the duration of neuron activity by measuring the whole peak width, left half peak width (peak rising fluorescence amplitude), and right half peak width (peak declining fluorescence amplitude) in individual calcium traces. In Figure 3d,e, we statistically analyzed the difference in whole peak width (resting-peakresting amplitude). We did not find statistical significance in the peak width in any of the three DA neuron populations cH  $(\chi_3^2 = 7.70; n = 404 \text{ [AL\_0.7]}, n = 386 \text{ [FD\_0.7]}, n = 361 \text{ [AL\_1.5]},$ n = 350 [FD\_1.5]; p = 0.052) (Figure 3d), iH ( $\chi_3^2 = 6.15$ ; n = 498[AL\_0.7], n = 485 [FD\_0.7], n = 449 [AL\_1.5], n = 424 [FD\_1.5]; p = 0.104) (Figure 3e) and in PT ( $\chi_3^2 = 5.50$ ; n = 521 [AL\_0.7],  $n = 498 \text{ [FD\_0.7]}, n = 491 \text{ [AL\_1.5]}, n = 379 \text{ [FD\_1.5]}; p = 0.138)$ (Figure 3f). Post hoc comparison did not show a significant change between AL and FD states in cH (median peak width:  $0.7\mu M$  [AL: 6.35 s; FD: 6.92 s], p = 1.000;  $1.5\mu M$  [AL: 6.13 s; FD: 6.51 s], p = 0.114), iH (median peak width: 0.7  $\mu$ M [AL: 5.96 s; FD: 5.98 s, p = 1.000;  $1.5 \mu \text{M}$  [AL: 5.69 s; FD: 6.08 s], p = 0.083), and PT (median peak width:  $0.7 \mu M$  [AL: 4.09 s; FD: 4.53 s], p = 0.177;  $1.5 \,\mu\text{M}$  [AL: 4.24s; FD: 4.29s], p = 1.000). All three DA neuron populations exhibited a mild but non-significant increase in peak amplitude in FD state post AMPH treatment in all doses.

Upon analyzing left half peak width in Figure 3g-i, which represents the time duration between resting and highest amplitude of the calcium peak, overall significant change was observed using Kruskal-Wallis ANOVA ( $\chi_3^2 = 16.61$ ; n = 404 $[AL_0.7]$ , n = 386  $[FD_0.7]$ , n = 361  $[AL_1.5]$ , n = 350  $[FD_1.5]$ ; p < 0.001) (Figure 3g) and post hoc comparison also showed significance between AL and FD groups at 1.5 µM dose only in cH (median peak width: 0.7 µM [AL: 0.82 s; FD: 0.79 s], p = 1.000; 1.5  $\mu$ M [AL: 0.72 s; FD: 0.85 s], p < 0.001). Similarly, significance was also found in iH neurons between two caloric states ( $\chi_3^2 = 24.91$ ; n = 498 [AL\_0.7], n = 485 [FD\_0.7], n = 449[AL\_1.5], n = 424 [FD\_1.5]; p < 0.001) with planned comparison indicating difference between physiological states at  $1.5 \,\mu\text{M}$  dose (median peak width:  $0.7 \,\mu\text{M}$  [AL:  $0.81 \,\text{s}$ ; FD:  $0.73 \,\text{s}$ ], p = 0.997; 1.5  $\mu$ M [AL: 0.71 s; FD: 0.83 s], p < 0.001) (Figure 3h). In PT neurons, although overall significant difference was observed ( $\chi_3^2 = 8.28$ ; n = 522 [AL\_0.7], n = 498 [FD\_0.7], n = 491[AL\_1.5], n = 379 [FD\_1.5]; p < 0.001), contrarily, post hoc test showed the difference between caloric states only at 0.7 µM

dose (median peak width:  $0.7 \mu M$  [AL: 0.80s; FD: 0.86s], p = 0.027;  $1.5 \mu M$  [AL: 0.83s; FD: 0.80s], p = 1.000; Figure 3i). In cH and iH neuron populations, significantly higher left half peak width was observed in FD groups post  $1.5 \mu M$  AMPH dose, whereas same trend was shown by PT neurons but at  $0.7 \mu M$  dose depicting the neuron activity to take significantly longer to reach the maximum amplitude.

The right-half peak width was analyzed to measure the time the calcium trace peak took to decline from the highest to its resting state. In Figure 3j, Kruskal-Wallis ANOVA test expressed the dosage effect in cH neurons ( $\chi_3^2 = 9.14$ ; n = 404 [AL\_0.7], n = 386[FD\_0.7], n=361 [AL\_1.5], n=350 [FD\_1.5]; p=0.028) and post hoc comparison revealed a significant difference between states at 1.5 µM dosage (median peak width: 0.7 µM [AL: 0.98 s; FD: 0.97 s], p = 1.000; 1.5  $\mu$ M [AL: 0.92 s; FD: 1.07 s], p = 0.016). Dose effect in iH neurons was also observed to be significant in Figure 3k ( $\chi_3^2 = 18.41$ ; n = 498 [AL\_0.7], n = 485 [FD\_0.7], n=449 [AL\_1.5], n=424 [FD\_1.5]; p<0.001). FD larvae exhibited a significant increase at 1.5 µM dosage when pairwise comparisons were done (median peak width: 0.7 µM [AL: 0.91 s; FD: 0.89 s, p = 1.000;  $1.5 \mu \text{M}$  [AL: 0.81 s; FD: 0.97 s], p < 0.001). Contrarily, significance was neither induced by dosage in PT neurons for right-hand peak width neurons ( $\chi_3^2 = 4.74$ ; n = 522[AL\_0.7], n = 498 [FD\_0.7], n = 491 [AL\_1.5], n = 378 [FD\_1.5]; p = 0.191) nor by post hoc comparison (median peak width:  $0.7 \mu M$  [AL: 0.96 s; FD: 1.01 s], p = 0.479; 1.5  $\mu M$  [AL: 0.97 s; FD: 1.05 s], p = 1.000) (Figure 31). Right-hand peak width data show that the FD state increased the time taken by the neuron activity to drift down from highest to resting amplitude causing the neuron activity to stay longer.

# 3.4 | Feeding States Impaired the Neuron Correlation Between DA Neuron Pairs Independently and Associatively With AMPH Doses

In Figure 4, we measured the dopamine neuron activity correlation between neuron pairs at baseline level (without AMPH) and two different doses. The correlation conveys how strongly the neuron activity is correlated between different DA neuron pairs and how feeding states and AMPH affect this correlation. Although the correlation coefficients calculated here are weak when their individual values were considered, we only made a relative comparison in this analysis. First, we compared the correlation between neuron pairs in both states at baseline level (Figure 4a,b). In the AL state (Figure 4a), we observed a significantly high correlation between all pairs. A relatively strong positive correlation was observed between cH-PT neuron activity (Spearman's R correlation: 0.1, p = 0.006), which was followed by the cH-iH pair (Spearman's R correlation: 0.086, p = 0.015); however, a negative correlation was shown by iH-PT neuron pair (Spearman's R correlation: -0.089, p = 0.021). Interestingly, when correlation was measured between neuron pairs in FD state (Figure 4b), although correlation coefficients were significant in between all pairs, we found a relatively stronger positive correlation between the iH-PT pair (Spearman's R correlation: 0.25, p < 0.001) which was contrary to the observation made in AL state. A relatively weak positive correlation was observed between the iH-cH pair (Spearman's R correlation: 0.21, p < 0.001), followed by a

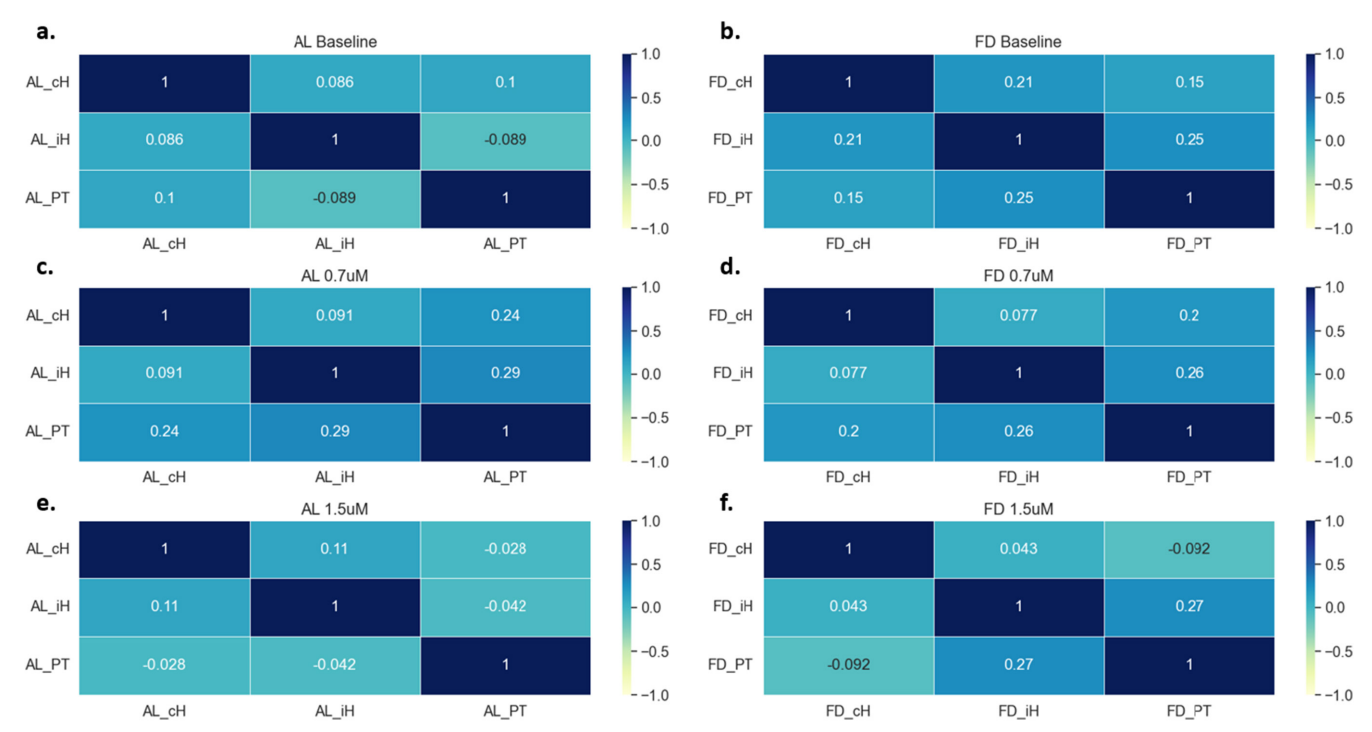


**FIGURE 4** | Calcium peak amplitude (df/f) correlation heatmap. Correlation analysis of DA neuron activity among all three DA populations in AL and FD states was performed in baseline and two AMPH doses. (a, b) Baseline: Neuron activity correlation between cH and PT was highest in AL larvae, followed by cH and iH neurons, whereas PT-iH neurons showed a negative correlation. FD larvae showed the highest neuron activity correlation between iH-PT neurons, followed by cH-iH neurons, and the least correlated pair was cH-PT. (c, d)  $0.7 \mu$ M: In the AL state, highly correlated pairs at lower AMPH doses were PT-iH and PT-cH, showing a noticeable increase at this dosage. cH-iH pairs were the least correlated here. Correlation in neuron activity in FD larvae showed an identical trend. (d, e)  $1.5 \mu$ M: At a higher AMPH dose of  $1.5 \mu$ M, cH-iH activity correlation in AL larvae was the highest among all DA populations. At this dosage, cH-PT and iH-PT neuron pairs showed a negative correlation in the activity. In the FD state, neuron activity was correlated between the iH-PT neuron pair followed by the cH-iH pair. Similar to the AL state, the FD state induced a negative correlation between the cH-PT pair.

weaker but significant positive correlation between the cH-PT pair (Spearman's R correlation: 0.15, p < 0.001).

When neuron activity correlation was measured in larvae after AMPH treatment, a significant change and reduction in correlation was observed in some pairs. In Figure 4c, when AL larvae were treated with 0.7 µM AMPH, iH neurons were strongly correlated with PT neurons (Spearman's R correlation: 0.29, p < 0.001). The positive correlation between cH and PT neurons was relatively weaker (Spearman's R correlation: 0.24, p < 0.001), and the least non-significant positive correlation was expressed by cH-iH pair (Spearman's R correlation: 0.091, p = 0.067). Larvae in the FD state treated with  $0.7 \mu M$  AMPH (Figure 4d) expressed a strong positive correlation between the iH-PT neuron pair (Spearman's R correlation: 0.26, p < 0.001). A significantly strong positive correlation was also observed in (Spearman's R correlation: 0.20, p < 0.001), and the least positive and non-significant correlation was exhibited by the cH-iH pair (Spearman's R correlation: 0.077, p = 1.000). At a higher AMPH dose (1.5 µM), neuron activity correlation between all neuron pairs in the AL state significantly reduced (Figure 4e). Strongest and significant positive correlation was seen between cH and iH (Spearman's R correlation: 0.11, p = 0.001). Activity correlation was found to be reduced and statistically non-significant between the cH-PT pair (Spearman's R correlation: -0.028, p = 0.560) and iH-PT neuron pair (Spearman's R correlation: -0.042, p=0.217). Contrary to the AL state, FD state post AMPH administration indicated the strongest positive correlation in this dosage in the iH-PT neuron pair (Spearman's R correlation: 0.27, p < 0.001), and the least positively correlated pair was iH-cH (Spearman's R correlation: 0.043, p = 0.893) and was non-significant. Between cH and PT neurons, similar to the AL state at 1.5  $\mu$ M dose, activity correlation was negative and significant (Spearman's R correlation: -0.092, p = 0.004).

# 3.5 | Feeding Affected the Calcium Spike Latency Dose-Dependently in Selective DA Populations

Latency in neuronal calcium spikes depicts the time elapsed between two subsequent adjacent peaks and possesses an inverse relationship with neuron activity frequency. We investigated neuron calcium trace latency and compared it pre- and post-AMPH at both doses and all three DA neuron populations. Interestingly, we found the outcomes contrary to what we saw in peak amplitude and width investigation dose-dependently. At  $0.7\,\mu\text{M}$  dose, we did see an overall significant change in latency after AMPH administration in cH neurons after Kruskal–Wallis ANOVA ( $\chi_3^2 = 16.11$ ; n = 391 [AL Baseline], n = 394 [AL\_0.7], n = 367 [FD Baseline], n = 376 [FD\_0.7]; p = 0.001) (Figure 5a). No significant latency change post-AMPH was observed except a mild increase in AL state and decrease in FD state (median difference: AL Baseline-AL\_0.7: 0.33 s, p = 0.618; FD Baseline-FD\_0.7:  $-0.11\,\text{s}$ , p = 1.000). However, at  $1.5\,\mu\text{M}$  dose

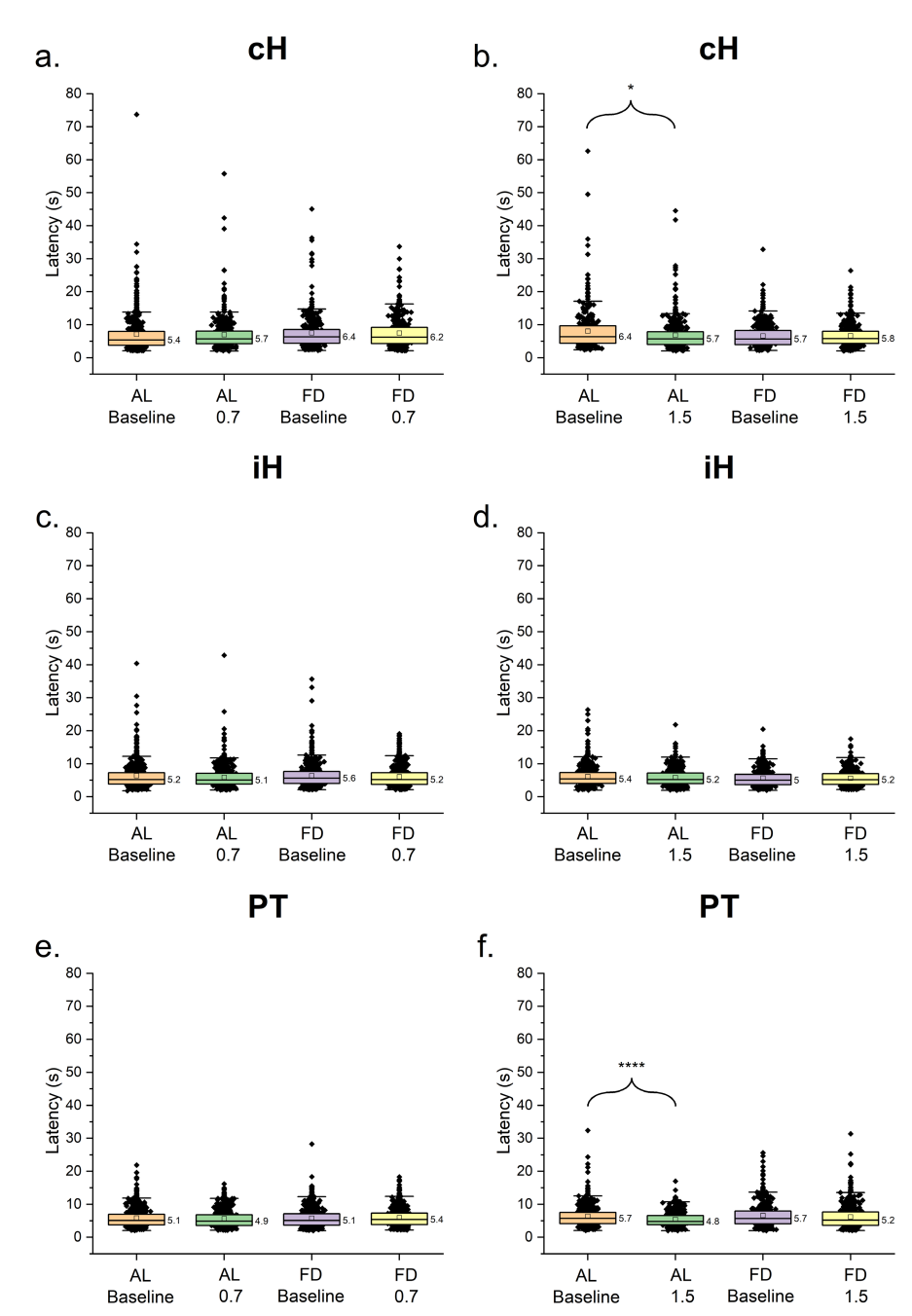


**FIGURE 5** | Inter-spike interval (Latency) comparison. Latency was statistically analyzed at two different doses of amphetamine (Baseline and  $0.7\mu$ M [AL: N=11; FD: N=10 fish] and Baseline and  $1.5\mu$ M [AL: N=9; FD: N=8 fish]) between paired subjects. Paired comparison between baselines and doses in AL and FD states using Kruskal–Wallis ANOVA for dependent data followed by Dunn's post hoc comparison. Pairwise comparisons were made between baselines and their respective doses in AL and FD states (pre- and post-AMPH) in all three DA neuron populations. (a, b) cH: Latency significantly decreased in cH neurons at  $1.5\mu$ M AMPH dose in AL state only (median difference: 0.15; p=0.021). (c, d) iH: No significant difference pre- and post-AMPH was observed in latency in iH neurons in both doses. (e, f) PT: Decreased latency was only observed in the AL state at  $1.5\mu$ M dose (median difference: 0.92; p<0.001) and remained non-significant everywhere else. Box plot limits are represented as Q1–Q3: 25%-75%, and whiskers are represented by outliers (1.5QR). The black horizontal line within the box represents the median with values mentioned on the right side of the line, and the blank square represents the mean of the data.

(Figure 5b), along with an overall significance with ANOVA ( $\chi_3^2$ =10.75; n=302 [AL Baseline], n=352 [AL\_1.5], n=348 [FD Baseline], n=342 [FD\_1.5]; p=0.013) planned comparison also showed a significant decrease in latency in cH neurons in AL state but a mild non-significant increase was observed in FD state (median difference: AL Baseline-AL\_1.5: -0.68 s, p=0.021; FD Baseline-FD\_1.5: 0.15 s, p=1.000). In Figure 5c,

iH neurons at  $0.7\,\mu\text{M}$  neither showed an overall significant effect of state ( $\chi_3^2$ =5.40; n=445 [AL Baseline], n=488 [AL\_0.7], n=448 [FD Baseline], n=475 [FD\_0.7]; p=0.147) nor latency change after AMPH treatment in both AL (median difference: AL Baseline-AL\_0.7:  $-0.13\,\text{s}$ , p=1.000; FD Baseline-FD\_0.7:  $-0.41\,\text{s}$ , p=0.407). Latency in iH neurons at  $1.5\,\mu\text{M}$  dose (Figure 5d) followed the same trend as it did at  $0.7\,\mu\text{M}$  dose.

Statistical significance was not observed either with ANOVA  $(\chi_3^2 = 5.86; n = 412 \text{ [AL Baseline]}, n = 440 \text{ [AL\_1.5]}, n = 405 \text{ [FD]}$ Baseline], n = 416 [FD\_1.5]; p = 0.118), and post hoc test in both caloric states (median difference: AL Baseline-AL\_1.5: -0.22s, p = 1.000; FD Baseline-FD\_1.5: 0.19 s, p = 1.000). PT neuron at  $0.7 \mu M$  dose did not express an overall significant change in latency  $(\chi_3^2 = 3.75; n = 490 \text{ [AL Baseline]}, n = 512 \text{ [AL\_0.7]}, n = 498$ [FD Baseline], n = 488 [FD\_0.7]; p = 0.288) (Figure 5e). Pairwise comparison also failed to show significance after AMPH administration (median difference: AL Baseline-AL\_0.7: -0.2s, p = 1.000; FD Baseline-FD\_0.7: 0.29 s, p = 1.000). PT neurons expressed a significant overall effect at 1.5  $\mu$ M ( $\chi_3^2 = 26.73$ ; n = 407[AL Baseline], n = 482 [AL\_1.5], n = 343 [FD Baseline], n = 371[FD\_0.7]; p < 0.001). Pairwise comparison indicated a significant decrease in latency in the AL state but not in the FD state (median difference: AL Baseline-AL\_1.5:  $-0.92 \,\mathrm{s}, p < 0.001$ ; FD Baseline-FD\_1.5:  $-0.45 \,\mathrm{s}$ , p = 0.188). The results showed a decrease in latency (increased neuron activity) when larvae were fully fed (AL state), indicating that food reward interferes with the rewarding properties of AMPH to induce a dosedependent change in DA neuron activity in these hypothalamic populations.

## 4 | Discussion

Using zebrafish larvae, this study investigated A11 (PT) and A14 (cH, iH) type dopamine (DA) neurons in the hypothalamus (Barrios et al. 2020; Haehnel-Taguchi et al. 2018). Generally, DA activity is influenced by the rewarding nature of food and drugs in the mesolimbic pathway, which initiates from the ventral tegmental area (VTA) and is projected into the nucleus accumbens (NAc), a part of the striatum in the mammalian brain (Holly and Miczek 2016). In zebrafish, research shows the innervations of DA neurons from the posterior tuberculum (PT) into the subpallium brain region in zebrafish, which is a teleost equivalent of mammalian striatum (Rink and Wullimann 2002). However, no evidence exists to identify the mammalian equivalent of the complete limbic reward pathway in the zebrafish brain. Moreover, how the interference of food and drug rewards affects the dopaminergic pathway has yet to be well understood. Thus, there is a considerable knowledge gap regarding the identification of reward circuitry in this animal model and the effects of complexing the drug reward with different feeding regimes on the known DA neuron populations. Therefore, to fill this gap, in this novel study, we evaluated the individual and interactive effects of food deprivation and different doses of amphetamine (AMPH) on three distinct dopaminergic regions in the hypothalamus of zebrafish larvae and compared the responses with Ad libitum fed larvae. Evidence shows that food-restriction and amphetamine increased excitability of dopamine neurons (Branch et al. 2013; Drevets et al. 2001). Thus, we hypothesized that dopamine neuron activity will increase in food-deprivation and its interaction with amphetamine. We found that hunger increased dopamine activity in all three dopamine regions both alone and interactively with amphetamine.

Zebrafish larvae are born with a yolk sac, which includes a supply of essential nutrition that serves as food only till 4 pdf and requires external feeding upon reaching 5 pdf (Sant and Timme-Laragy 2018). We used 6dpf larvae with an 18-h acute overnight

food-deprivation period to obtain dopaminergic activity recordings. According to our findings, food deprivation alone increased neuron activity in all three DA populations. Our results agree with the outcomes in the previous studies that were performed in acutely fasted rodents and acute central ghrelin injection (Anderberg et al. 2016; Roseberry 2015). Dopaminergic neurons receive synapses from various neuron populations in the brain (Watabe-uchida et al. 2012). One such neuron population is Agouti-related protein/Neuropeptide-Y (AgRP/NPY) neurons in the hypothalamus, which get stimulated when ghrelin (a gut hormone that is secreted during starvation) binds to its receptors on AgRP/NPY neuron surface (Essner et al. 2017; Khelifa, Skov, and Holst 2021). Food deprivation increases AgRP/NPY mRNA expression (Bi, Robinson, and Moran 2003). In addition, the direct incremental effect of ghrelin on dopaminergic neurons has been observed via its binding onto ghrelin receptors (Abizaid 2009; Jerlhag and Egecioglu 2010; Quarta et al. 2009). These results altogether indicate that A11 and A14 DA populations are affected by hunger and probably receive synaptic inputs directly or indirectly from AgRP/NPY neurons and are also affected by ghrelin release. Thus, the presence of AgRP/NPY innervations in and ghrelin receptors on zebrafish A11 and A14 neurons can be investigated in the future.

We also reported that neuron activity amplitude was relatively higher in the FD state than in the AL state with both doses and was comparatively greater with the higher dose in all three DA populations. Food deprivation and AMPH-mediated increase in DA neuron activity could have arisen from decreased insulin levels in FD states. The studies show that dexamethasone (an insulin blocker) injection and food deprivation independently increase NPY mRNA expression, and FD-mediated NPY release increases DA activity (Rezitis, Herzog, and Kin 2022; Sato et al. 2005). In mice, amphetamine treatment significantly decreases fasting blood glucose, and reduced blood glucose further lowers insulin levels (Fruehwald-schultes et al. 2000; Zhang et al. 2018). Although studies in the context of insulin-hunger-AMPH are scarce, especially in zebrafish, more than 70% of glucose and insulin regulatory genes studied in zebrafish and humans are conserved and show a similar regulation pathway (Zhang et al. 2018). Thus, the reduction in insulin caused by food deprivation and its further decrease by AMPH treatment might have led to an increase in NPY levels, which probably caused a surge in DA activity in FD larvae. Investigating the connection among glucose, insulin, food deprivation, and amphetamine can shed more light on their collective impact on DA activity in mammals and zebrafish. The aforementioned study showing the innervation of DA neurons from PT into the subpallium and the increase in dopaminergic neuron activity in PT along with cH and iH in FD states points to PT being the primary rewardrelated region. From our findings and these previous observations, it would be reasonable to assume that the differences in brain structure may have functionally compensated for the rewarding properties by providing a part of the central rewarding function to the PT-striatum circuitry in this teleost. However, this assumption holds unless the reward-related DA populations are identified. Despite the limited study of cH and iH DA neuronal projections, an increase in their activity also points to their vet unknown innervations into the zebrafish striatum besides PT DA neurons and could be explored in the future to understand their function in eliciting hedonic reward.

In the AL and FD states, we performed df/f correlation analysis between DA neuron pairs pre- and post-AMPH treatment. The baseline calcium activity (df/f) correlation between all DA pairs, both within the A14 neurons and between A14 and A11 neurons, was relatively higher in the FD state than in the Ad libitum state. A11 neurons receive inputs from several nuclei, including the parabrachial nucleus (PBN), which is important in modulating feeding-related homeostasis (Koblinger et al. 2014; Zhao et al. 2023). In zebrafish, the secondary gustatory-general viscerosensory nucleus (SGN/V) is present as the mammalian equivalent of PBN containing food/taste sensory neurons and projects into the regions of the posterior tuberculum (Henriques et al. 2019; Yáñez et al. 2022). Here, calretinin (CR) is expressed predominantly in SGN, which is a part of the periventricular hypothalamus in PT and caudal/ intermediate hypothalamic regions in zebrafish brains, and food deprivation increases its expression (Hua et al. 2018; Mueller 2012). The studies show that the presence of CR in striatal DA neurons in different animal species exhibits various effects of CR in DA neurons and its precursor L-DOPA (Isaacs, Wolpoe, and Jacobowitz 1997; Mura, Feldon, and Mintz 2000; Petryszyn et al. 2016). Yet, the effects of CR on DA excitability remained largely unexplored. Dopaminergic activity is also affected by AgRP neurons, and in the zebrafish brain, AgRP neurons are located in the periventricular hypothalamus while projecting throughout the hypothalamic regions (Shainer et al. 2017). Additionally, hypothalamic AgRP neurons are relatively closer to A14 neurons. Therefore, an increase in DA activity simultaneously via SGN-CR in A11 and AgRP in both A11 and A14 DA neurons could be a possible reason for the relatively higher correlation in activity between both DA types in food deprivation. Calcitonin gene-related peptide (CGRP) is a gut protein that is present in both mammals and zebrafish, and its expressive neurons are present in PBN and A11 neurons in mammals (Kuil et al. 2021; Milet et al. 2018; Zhao et al. 2023). CGRP has been shown to suppress food intake in animals in fed states (Sanford et al. 2019). This suggests that the fed state might have induced the release of CGRP, and it also increases DA neuron activity either directly from A11 neurons or via a neuron pathway other than CR (Rahimi, Sajedianfard, and Owji 2017). Contrarily, a recent study showed that ablation of AgRP neurons led to the impairment of dopaminergic neuron activity in rodents, and AgRP neuron activity generally decreases in the fed state (Reichenbach et al. 2022). This contradictory activity in dopaminergic neurons in the A11 and A14 regions may have led to a decrease in correlation relative to what we have observed in the FD state.

More interestingly, with AMPH treatment, the activity correlation increased in the AL state relative to the FD state at both doses, and the increment was relatively more noticeable at the higher dose. This altered correlation from amphetamine treatment could stem from its effect on a peptide called protein kinase C (PKC) in PBN that mediates taste transduction (Varkevisser and Kinnamon 2023). Research shows that both food and amphetamine increase PKC activity, and an independent study shows a PKC-mediated increase in dopamine activity (Inoguchi et al. 1939; Krivanek 1997; Mutanen et al. 2000). However, food and AMPH both have been shown to inhibit AgRP neuron activity, and AgRP ablation decreased

dopamine neuron excitation in rodents (Alhadeff et al. 2019; Reichenbach et al. 2022). These two findings are contradictory, but identical modulation in PKC and AgRP-mediated conditions express an increased correlation in the AL state. The function of PKC has been identified in zebrafish only recently for its involvement in fat and glucose metabolism (Sun et al. 2021). Hence, there is a need to perform further studies about its participation in modulating DA neuron activity along with the use of stimulants. Moreover, the difference in activity correlation within and between neuron populations also showcases the ability of feeding states to leverage different pathways in modulating the neuron activity correlation. This can be observed especially when activity between iH and PT in the FD state exhibited the highest correlation; it went to its lowest negative value in the AL baseline state and in both AL and FD states at higher AMPH doses.

The results presented in this novel study feature the ability of hunger and its interaction with amphetamine to significantly affect the reward-related neuron populations in the teleost brain. Moreover, it broadly confirms the functional conservation of dopamine activity across different animal species. Our results show that the dopaminergic neurons exhibited increased activity in all three hypothalamic populations when subjected to acute fasting alone and with AMPH treatment relative to the fed state. Exploring this cohesive effect of caloric state-AMPH on DA neurons further could help devise interventional strategies for controlling the DA activity by varying diet and stimulant doses. The caloric state-AMPH treatment also altered the correlation between populations. This outcome could be useful to understand how different DA populations communicate when subjected to rewarding stimuli.

# 5 | Conclusion

In this novel research, we showed the change in dopamine activity firing in three regions of hypothalamus in 6dpf zebrafish larva when subjected to food-deprivation and amphetamine. We investigated the peak amplitude (fluorescence change), single calcium trace duration (peak width), peak rising and peak falling time in the regions. Our findings show that dopamine activity was enhanced by hunger. After AMPH treatment, increase in DA activity was dose dependent in different regions. Furthermore, we measured the effects of hunger and AMPH on the peak amplitude correlation between inter and intra DA populations. The activity was highly correlated in food deprived state relative to fed state and correlation was disrupted by amphetamine treatment. Finally, we analyzed peak latency representing the frequency of the calcium trace occurrence in drugged larvae subjected to starvation where traces were frequently observed in fed state. Overall, our findings show that the teleost DA neuron activity subject to an AMPH dose-dependent change and the drug evoked an increase in their activity when it interacted with starvation state.

# **Author Contributions**

Conceptualization, funding acquisition, resources, supervision: Erica E. Jung; methodology: Erica E. Jung and Pushkar Bansal; investigation, Formal Analysis: Erica E. Jung and Pushkar Bansal; visualization:

Pushkar Bansal; writing: Erica E. Jung, Mitchell F. Roitman and Pushkar Bansal; original draft: Pushkar Bansal; review and editing: Erica E. Jung and Mitchell F. Roitman.

## Acknowledgments

We thank Dr. Adam Douglass for providing the Tg(th2:GCaMP7s) transgenic line. We also thank John Jutoy for helping with fish room maintenance.

## **Conflicts of Interest**

The authors declare no conflicts of interest.

#### **Data Availability Statement**

The data will be made available from the corresponding author upon reasonable request.

## **Peer Review**

The peer review history for this article is available at https://www.webof science.com/api/gateway/wos/peer-review/10.1002/jnr.25396.

# **Declaration of Transparency**

The authors, reviewers, and editors affirm that in accordance to the policies set by the *Journal of Neuroscience Research*, this manuscript presents an accurate and transparent account of the study being reported and that all critical details describing the methods and results are present.

## References

Abizaid, A. 2009. "Ghrelin and Dopamine: New Insights on the Peripheral Regulation of Appetite." *Journal of Neuroendocrinology* 21, no. 9: 787–793.

Alhadeff, A. L., N. Goldstein, O. Park, M. L. Klima, A. Vargas, and J. N. Betley. 2019. "Natural and Drug Rewards Engage Distinct Pathways That Converge on Coordinated Hypothalamic and Reward Circuits." *Neuron* 103, no. 5: 891–908.e6. https://doi.org/10.1016/j.neuron.2019.05.050.

Anderberg, R. H., C. Hansson, M. Fenander, et al. 2016. "The Stomach-Derived Hormone Ghrelin Increases Impulsive Behavior." *Neuropsychopharmacology* 41, no. 5: 1199–1209. https://doi.org/10.1038/npp.2015.297.

Bansal, P., M. F. Roitman, and E. E. Jung. 2023. "Caloric State Modulates Locomotion, Heart Rate and Motor Neuron Responses to Acute Administration of d-Amphetamine in Zebrafish Larvae." *Physiology and Behavior* 264, no. March: 114144. https://doi.org/10.1016/j.physbeh. 2023.114144.

Barrios, J. P., W. C. Wang, R. England, E. Reifenberg, and A. D. Douglass. 2020. "Hypothalamic Dopamine Neurons Control Sensorimotor Behavior by Modulating Brainstem Premotor Nuclei in Zebrafish." *Current Biology* 30, no. 23: 4606–4618.e4. https://doi.org/10.1016/j.cub. 2020.09.002.

Bernardini, G. L., X. Gu, E. Viscardi, et al. 1991. "Amphetamine-Induced and Spontaneous Release of Dopamine from A9 and A10 Cell Dendrites: An in Vitro Electrophysiological Study in the Mouse." *Journal of Neural Transmission* 84: 183–193. https://doi.org/10.1007/BF01244969.

Bi, S., B. M. Robinson, and T. H. Moran. 2003. "Acute Food Deprivation and Chronic Food Restriction Differentially Affect Hypothalamic NPY mRNA Expression." *American Journal of Physiology. Regulatory, Integrative and Comparative Physiology* 285, no. 5 54–5: 1030–1036. https://doi.org/10.1152/ajpregu.00734.2002.

Björklund, A., and S. B. Dunnett. 2007. "Dopamine Neuron Systems in the Brain: An Update." *Trends in Neurosciences* 30, no. 5: 194–202. https://doi.org/10.1016/j.tins.2007.03.006.

Branch, S. Y., R. B. Goertz, A. L. Sharpe, et al. 2013. "Food Restriction Increases Glutamate Receptor-Mediated Burst Firing of Dopamine Neurons." *Journal of Neuroscience* 33, no. 34: 13861–13872. https://doi.org/10.1523/JNEUROSCI.5099-12.2013.

Calipari, E. S., and M. J. Ferris. 2013. "Amphetamine Mechanisms and Actions at the Dopamine Terminal Revisited." *Journal of Neuroscience* 33, no. 21: 8923–8925. https://doi.org/10.1523/JNEUROSCI.1033-13.2013.

Campbell, B. A., and H. C. Fibiger. 1971. "Potentiation of Amphetamine-Induced Arousal by Starvation." *Nature* 233, no. 5319: 424–425. https://doi.org/10.1038/233424a0.

Capsoni, S., A. Fogli Iseppe, F. Casciano, and A. Pignatelli. 2021. "Unraveling the Role of Dopaminergic and Calretinin Interneurons in the Olfactory Bulb." *Frontiers in Neural Circuits* 15: 718221. https://doi.org/10.3389/fncir.2021.718221.

Charbit, A. R., S. Akerman, P. R. Holland, and P. J. Goadsby. 2009. "Neurons of the Dopaminergic/Calcitonin Gene-Related Peptide A11 Cell Group Modulate Neuronal Firing in the Trigeminocervical Complex: An Electrophysiological and Immunohistochemical Study." *Journal of Neuroscience* 29, no. 40: 12532–12541. https://doi.org/10.1523/JNEUROSCI.2887-09.2009.

Clemens, S., D. Rye, and S. Hochman. 2006. "Restless Legs Syndrome: Revisiting the Dopamine Hypothesis from the Spinal Cord Perspective." *Neurology* 67, no. 1: 125–130. https://doi.org/10.1212/01.wnl.00002 23316.53428.c9.

Cone, J. J., J. E. Mccutcheon, and M. F. Roitman. 2014. "Ghrelin Acts as an Interface Between Physiological State and Phasic Dopamine Signaling." *Journal of Neuroscience* 34, no. 14: 4905–4913. https://doi.org/10.1523/JNEUROSCI.4404-13.2014.

Deroche, V., P. V. Piazza, P. Casolini, M. Le Moal, and H. Simon. 1993. "Sensitization to the Psychomotor Effects of Amphetamine and Morphine Induced by Food Restriction Depends on Corticosterone Secretion." *Brain Research* 611, no. 2: 352–356. https://doi.org/10.1016/0006-8993(93)90526-S.

Di Chiara, G., and A. Imperato. 1988. "Drugs Abused by Humans Preferentially Increase Synaptic Dopamine Concentrations in the Mesolimbic System of Freely Moving Rats." *Proceedings of the National Academy of Sciences of the United States of America* 85, no. 14: 5274–5278. https://doi.org/10.1073/pnas.85.14.5274.

Drevets, W. C., C. Gautier, J. C. Price, et al. 2001. "Amphetamine-Induced Dopamine Release in Human Ventral Striatum Correlates with Euphoria." *Biological Psychiatry* 3223: 81–96.

Engelhard, B., J. Finkelstein, J. Cox, et al. 2019. "Specialized Coding of Sensory, Motor and Cognitive Variables in VTA Dopamine Neurons." *Nature* 570, no. 7762: 509–513. https://doi.org/10.1038/s41586-019-1261-9.

Essner, R. A., A. G. Smith, A. A. Jamnik, A. R. Ryba, Z. D. Trutner, and M. E. Carter. 2017. "AgRP Neurons Can Increase Food Intake During Conditions of Appetite Suppression and Inhibit Anorexigenic Parabrachial Neurons." *Journal of Neuroscience* 37, no. 36: 8678–8687. https://doi.org/10.1523/JNEUROSCI.0798-17.2017.

Fiorenzano, A., E. Sozzi, M. Parmar, and P. Storm. 2021. "Dopamine Neuron Diversity: Recent Advances and Current Challenges in Human Stem Cell Models and Single Cell Sequencing." *Cells* 10, no. 6: 1366. https://doi.org/10.3390/cells10061366.

Fougère, M., A. Flaive, A. Frigon, and D. Ryczko. 2019. "Descending Dopaminergic Control of Brainstem Locomotor Circuits." *Current Opinion in Physiology* 8: 30–35. https://doi.org/10.1016/j.cophys.2018. 12.004.

Fruehwald-schultes, B., W. Kern, J. Born, H. L. Fehm, and A. Peters. 2000. "Comparison of the Inhibitory Effect of Insulin and Hypoglycemia on Insulin Secretion in Humans." *Metabolism* 49, no. 7: 950–953. https://doi.org/10.1053/mt.2000.6757.

Geisler, C. E., and M. R. Hayes. 2023. "Metabolic Hormone Action in the VTA: Reward-Directed Behavior and Mechanistic Insights." *Physiology and Behavior* 268: 114236. https://doi.org/10.1016/j.physbeh.2023. 114236.

Giros, B., M. Jaber, S. R. Jones, R. M. Wightman, and M. G. Caron. 1996. "Hyperlocomotion and Indifference to Cocaine and Amphetamine in Mice Lacking the Dopamine Transporter." *Nature* 379, no. 6566: 606–612. https://doi.org/10.1038/379606a0.

Haehnel-Taguchi, M., A. M. Fernandes, M. Böhler, I. Schmitt, L. Tittel, and W. Driever. 2018. "Projections of the Diencephalospinal Dopaminergic System to Peripheral Sense Organs in Larval Zebrafish (Danio Rerio)." *Frontiers in Neuroanatomy* 12: 20. https://doi.org/10.3389/fnana.2018.00020.

Henriques, P. M., N. Rahman, S. E. Jackson, and I. H. Bianco. 2019. "Nucleus Isthmi is Required to Sustain Target Pursuit During Visually Guided Prey-Catching." *Current Biology* 29, no. 11: 1771–1786.e5. https://doi.org/10.1016/j.cub.2019.04.064.

Holly, E. N., and K. A. Miczek. 2016. "Ventral tegmental area dopamine revisited: effects of acute and repeated stress." *Psychopharmacology* 233: 163–186. https://doi.org/10.1007/s00213-015-4151-3.

Hua, R., X. Wang, X. Chen, et al. 2018. "Calretinin Neurons in the Midline Thalamus Modulate Starvation-Induced Arousal Article Calretinin Neurons in the Midline Thalamus Modulate Starvation-Induced Arousal." *Current Biology* 28, no. 24: 3948–3959.e4. https://doi.org/10.1016/j.cub.2018.11.020.

Ikemoto, S. 2010. "Brain Reward Circuitry Beyond the Mesolimbic Dopamine System: A Neurobiological Theory." *Neuroscience and Biobehavioral Reviews* 35, no. 2: 129–150. https://doi.org/10.1016/j.neubiorev.2010.02.001.

Inoguchi, T., P. Li, F. Umeda, et al. 1939. "High Glucose Level and Free Fatty Acid Stimulate Protein Kinase C – Dependent Activation of NAD (P) H Oxidase in Cultured Vascular Cells." *Diabetes* 49: 1939–1945.

Isaacs, K. R., M. E. Wolpoe, and D. M. Jacobowitz. 1997. "Calretinin-Immunoreactive Dopaminergic Neurons from Embryonic Rat Mesencephalon Are Resistant to Levodopa-Induced Neurotoxicity." *Experimental Neurology* 32, no. 146: 25–32.

Jerlhag, E., and E. Egecioglu. 2010. "Ghrelin Receptor Antagonism Attenuates Cocaine- and Amphetamine-Induced Locomotor Stimulation, Accumbal Dopamine Release, and Conditioned Place Preference." *Drug and Alcohol Dependence* 211: 415–422. https://doi.org/10.1007/s00213-010-1907-7.

Kappel, J. M., D. Förster, K. Slangewal, et al. 2022. "Visual Recognition of Social Signals by a Tectothalamic Neural Circuit." *Nature* 608, no. 7921: 146–152. https://doi.org/10.1038/s41586-022-04925-5.

Keller, P. J., and M. B. Ahrens. 2015. "Visualizing Whole-Brain Activity and Development at the Single-Cell Level Using Light-Sheet Microscopy." *Neuron* 85, no. 3: 462–483. https://doi.org/10.1016/j.neuron.2014.12.039.

Khelifa, M. S., L. J. Skov, and B. Holst. 2021. "Biased Ghrelin Receptor Signaling and the Dopaminergic System as Potential Targets for Metabolic and Psychological Symptoms of Anorexia Nervosa." *Frontiers in Endocrinology (Lausanne)* 12: 734547.

Kim, D. H., J. Kim, J. C. Marques, et al. 2017. "Pan-Neuronal Calcium Imaging With Cellular Resolution in Freely Swimming Zebrafish." *Nature Methods* 14, no. 11: 1107–1114. https://doi.org/10.1038/nmeth.4429.

Koblinger, K., T. Füzesi, J. Ejdrygiewicz, A. Krajacic, J. S. Bains, and P. J. Whelan. 2014. "Characterization of A11 Neurons Projecting to the

Spinal Cord of Mice." *PLoS One* 9, no. 10: e109636. https://doi.org/10. 1371/journal.pone.0109636.

Koirala, S., S. Shah, and L. Khanal. 2014. "Effect of D-Amphetamine on Dopaminergic Neurons of Substantia Nigra and Expression of Tyrosine Hydroxylase in Striatum and Pre-Frontal Cortex of D-Amphetamine Treated Wistar Rats." *Russian Open Medical Journal* 3, no. 4: 0401. https://doi.org/10.15275/rusomj.2014.0401.

Korchynska, S., P. Rebernik, M. Pende, et al. 2022. "A Hypothalamic Dopamine Locus for Psychostimulant-Induced Hyperlocomotion in Mice." *Nature Communications* 13, no. 1: 5944. https://doi.org/10.1038/s41467-022-33584-3.

Kossack, M. E., and B. W. Draper. 2019. "Genetic Regulation of Sex Determination and Maintenance in Zebrafish (Danio Rerio)." *Current Topics in Developmental Biology* 134: 119–149. https://doi.org/10.1016/bs.ctdb.2019.02.004.

Kramer, J. C., V. S. Fischman, and D. C. Littlefield. 1967. "Amphetamine Abuse: Pattern and Effects of High Doses Taken Intravenously." *JAMA* 201, no. 5: 305–309. https://doi.org/10.1001/jama.1967.03130050039011.

Krivanek, J. 1997. "Protein Kinase C in the Parabrachial Nucleus of Rats During Conditioned Taste Aversion Induced by Amphetamine." *Neuroscience Letters* 236: 17–20.

Kuil, L. E., R. K. Chauhan, W. W. Cheng, and R. M. W. Hofstra. 2021. "Zebrafish: A Model Organism for Studying Enteric Nervous System Development and Disease." *Frontiers in Cell and Developmental Biology* 8, no. January: 1–15. https://doi.org/10.3389/fcell.2020.629073.

Liu, S., and S. L. Borgland. 2015. "Regulation of the Mesolimbic Dopamine Circuit by Feeding Peptides." *Neuroscience* 289: 19–42. https://doi.org/10.1016/j.neuroscience.2014.12.046.

Milet, A., R. Parlato, J. Rouzeau, et al. 2018. "Neurons of the Dopaminergic/Calcitonin Gene-Related Peptide A11 Cell Group Modulate Neuronal Firing in the Trigeminocervical Complex: An Electrophysiological and Immunohistochemical Study." *Journal of Comparative Neurology* 12, no. 10: 1–15. https://doi.org/10.1002/cne. 25020.

Morales, M., and E. B. Margolis. 2017. "Ventral Tegmental Area: Cellular Heterogeneity, Connectivity and Behaviour." *Nature Reviews Neuroscience* 18, no. 2: 73–85. https://doi.org/10.1038/nrn.2016.165.

Mueller, T. 2012. "What Is the Thalamus in Zebrafish?" *Frontiers in Neuroscience* 6, no. May: 1–14. https://doi.org/10.3389/fnins.2012.00064.

Mura, A., J. Feldon, and M. Mintz. 2000. "The Expression of the Calcium Binding Protein Calretinin in the Rat Striatum: Effects of Dopamine Depletion and L-DOPA Treatment." *Experimental Neurology* 332: 322–332. https://doi.org/10.1006/exnr.2000.7441.

Mutanen, M., A. Pajari, S. Oikarinen, and S. Gra. 2000. "Diets Enriched with Cereal Brans or Inulin Modulate Protein Kinase C Activity and Isozyme Expression in Rat Colonic Mucosa." *British Journal of Nutrition* 84: 635–643.

Petryszyn, S., T. Di, A. Parent, and M. Parent. 2016. "Neurobiology of Disease the Number of Striatal Cholinergic Interneurons Expressing Calretinin Is Increased in Parkinsonian Monkeys." *Neurobiology of Disease* 95: 46–53. https://doi.org/10.1016/j.nbd.2016.07.002.

Phillips, R. A., J. J. Tuscher, S. L. Black, et al. 2022. "An Atlas of Transcriptionally Defined Cell Populations in the Rat Ventral Tegmental Area." *Cell Reports* 39, no. 1: 110616. https://doi.org/10.1016/j.celrep. 2022.110616.

Quarta, D., C. Di Francesco, S. Melotto, L. Mangiarini, C. Heidbreder, and G. Hedou. 2009. "Rapid Communication: Systemic Administration of Ghrelin Increases Extracellular Dopamine in the Shell but Not the Core Subdivision of the Nucleus Accumbens." *Neurochemistry International* 54, no. 2: 89–94.

Rahimi, K., J. Sajedianfard, and A. A. Owji. 2017. "The Effect of Intracerebroventricular Injection of CGRP on Pain Behavioral Responses and Monoamines Concentrations in the Periaqueductal Gray Area in rat." *Iranian Journal of Basic Medical Sciences* 21: 395–399. https://doi.org/10.22038/IJBMS.2018.26384.6467.

Reichenbach, A., R. E. Clarke, R. Stark, et al. 2022. "Metabolic Sensing in AgRP Neurons Integrates Homeostatic State with Dopamine Signalling in the Striatum." *eLife* 11: 72668.

Rezitis, J., H. Herzog, and C. Kin. 2022. "Neuropeptide Y Interaction With Dopaminergic and Serotonergic Pathways: Interlinked Neurocircuits Modulating Hedonic Eating Behaviours." *Progress in Neuropsychopharmacology and Biological Psychiatry* 113, no. April 2021: 110449. https://doi.org/10.1016/j.pnpbp.2021.110449.

Rink, E., and M. F. Wullimann. 2002. "Connections of the Ventral Telencephalon and Tyrosine Hydroxylase Distribution in the Zebrafish Brain (Danio Rerio) Lead to Identification of an Ascending Dopaminergic System in a Teleost." *Brain Research Bulletin* 57, no. 3–4: 385–387. https://doi.org/10.1016/S0361-9230(01)00696-7.

Roseberry, A. G. 2015. "Acute Fasting Increases Somatodendritic Dopamine Release in the Ventral Tegmental Area." *Journal of Neurophysiology* 114, no. 2: 1072–1082. https://doi.org/10.1152/jn.01008.2014.

Ryczko, D., and R. Dubuc. 2017. "Dopamine and the Brainstem Locomotor Networks: From Lamprey to Human." *Frontiers in Neuroscience* 11: 295. https://doi.org/10.3389/fnins.2017.00295.

Sanford, D., L. Luong, A. Gabalski, et al. 2019. "An Intraperitoneal Treatment with Calcitonin Gene-Related Peptide (CGRP) Regulates Appetite, Energy Intake/Expenditure, and Metabolism." *Journal of Molecular Neuroscience* 67, no. 1: 28–37. https://doi.org/10.1007/s12031-018-1202-3.

Sant, K. E., and A. R. Timme-Laragy. 2018. "Zebrafish as a Model for Toxicological Perturbation of Yolk and Nutrition in the Early Embryo." *Current Environmental Health Reports* 5, no. 1: 125–133. https://doi.org/10.1007/s40572-018-0183-2.

Sato, I., H. Arima, N. Ozaki, et al. 2005. "Insulin Inhibits Neuropeptide Y Gene Expression in the Arcuate Nucleus Through GABAereic Systems." *Journal of Neuroscience* 25, no. 38: 8657–8664. https://doi.org/10.1523/JNEUROSCI.2739-05.2005.

Schultz, W. 2002. "Getting Formal With Dopamine and Reward." *Neuron* 36: 241–263.

Shainer, I., A. Buchshtab, T. A. Hawkins, S. W. Wilson, and R. D. Cone. 2017. "Novel Hypophysiotropic AgRP2 Neurons and Pineal Cells Revealed by BAC Transgenesis in Zebrafish." *Science Reports* 7: 44777. https://doi.org/10.1038/srep44777.

Siciliano, C. A., E. S. Calipari, M. J. Ferris, and S. R. Jones. 2014. "Biphasic Mechanisms of Amphetamine Action at the Dopamine Terminal." *Journal of Neuroscience* 34, no. 16: 5575–5582. https://doi.org/10.1523/JNEUROSCI.4050-13.2014.

Sun, S., X. Cao, L. F. C. Castro, Ó. Monroig, and J. Gao. 2021. "A Network-Based Approach to Identify Protein Kinases Critical for Regulating srebf1 in Lipid Deposition Causing Obesity." *Functional & Integrative Genomics* 21: 557–570. https://doi.org/10.1007/s10142-021-00798-5.

Varkevisser, B., and S. U. E. C. Kinnamon. 2023. "Sweet Taste Transduction in Hamster: Role of Protein Kinases." *Journal of Neurophysiology* 83: 2526–2532.

Vezina, P. 1988. "Amphetamine Injected Into the Ventral Tegmental Area Sensitizes the Nucleus Accumbens Dopaminergic Response to Systemic Amphetamine: An In Vivo Microdialysis Study in the Rat." *Brain research* 245: 332–337.

Wasel, O., and J. L. Freeman. 2020. "Chemical and Genetic Zebrafish Models to Define Mechanisms of and Treatments for Dopaminergic

Neurodegeneration." *International Journal of Molecular Sciences* 21, no. 17: 1–14. https://doi.org/10.3390/ijms21175981.

Watabe-uchida, M., L. Zhu, S. K. Ogawa, A. Vamanrao, and N. Uchida. 2012. "Article Whole-Brain Mapping of Direct Inputs to Midbrain Dopamine Neurons." *Neuron* 74, no. 5: 858–873. https://doi.org/10.1016/j.neuron.2012.03.017.

Wei, C., X. Han, D. Weng, et al. 2018. "Response Dynamics of Midbrain Dopamine Neurons and Serotonin Neurons to Heroin, Nicotine, Cocaine, and MDMA." *Cell Discovery* 4, no. 1: 60. https://doi.org/10.1038/s41421-018-0060-z.

Wilson, C., G. G. Nomikos, M. Collu, and H. C. Fibiger. 1995. "Dopaminergic Correlates of Motivated Behavior: Importance of Drive." *Journal of Neuroscience* 15, no. 7: 5169–5178.

Yáñez, J., M. Folgueira, I. Lamas, and R. Anadón. 2022. "The Organization of the Zebrafish Pallium From a Hodological Perspective." *Journal of Comparative Neurology* 530, no. 8: 1164–1194. https://doi.org/10.1002/cne.25268.

Ye, Q., J. Nunez, and X. Zhang. 2023. "Zona incerta dopamine neurons encode motivational vigor in food seeking." *Science Advances* 9: eadi5326. https://www.science.org.

Zhang, X., and A. N. Van Den Pol. 2016. "Hypothalamic Arcuate Nucleus Tyrosine Hydroxylase Neurons Play Orexigenic Role in Energy Homeostasis." *Nature Neuroscience* 19, no. 10: 1341–1347. https://doi.org/10.1038/nn.4372.

Zhang, Y., C. Qin, L. Yang, R. Lu, X. Zhao, and G. Nie. 2018. "A Comparative Genomics Study of Carbohydrate/Glucose Metabolic Genes: From Fish to Mammals." *BMC Genomics* 19, no. 1: 246. https://doi.org/10.1186/s12864-018-4647-4.

Zhang, Y., G. Shu, Y. Bai, J. Chao, X. Chen, and H. Yao. 2018. "Effect of Methamphetamine on the Fasting Blood Glucose in Methamphetamine Abusers." *Metabolic Brain Disease* 33, no. 5: 1585–1597. https://doi.org/10.1007/s11011-018-0265-8.

Zhao, Z., Y. Chen, Y. Xuan, G. Zhou, and W. Qiu. 2023. "Parabrachial Nucleus Neuron Circuits That Control Feeding Behavior and Energy Balance." *Obesity Medicine* 42, no. August: 100509. https://doi.org/10.1016/j.obmed.2023.100509.

# **Supporting Information**

Additional supporting information can be found online in the Supporting Information section.